

Atmospheric Corrosion Behaviour and Degradation of High-Strength Bolt in Marine and Industrial Atmosphere Environments

Xiaokui Yang^{1,2}, Lunwu Zhang^{1,2,*}, Shiyan Zhang^{1,2}, Kun Zhou^{1,2}, Ming Li³, Qiongyao He^{1,2}, Jingcheng Wang^{1,2}, Shuai Wu^{1,2}, Huaming Yang^{1,2}

¹ Southwest Technology and Engineering Research Institute, Chongqing 400039, P. R. China

² Chongqing Key Laboratory of Environmental Effect and Protection, Chongqing 400039, P. R. China

³ Avic China Aero-polytechnology Establishment, Beijing 100095, P. R. China

*E-mail: zhangsteri@yeah.net

Received: 18 September 2020 / Accepted: 8 November 2020 / Published: 30 November 2020

The atmospheric corrosion behaviour and properties degradation law of 1Cr17Ni2 high-strength bolt exposed in marine and industrial atmosphere environments up to 36 months were investigated in virtue of scanning electron microscope (SEM), energy dispersive spectroscopy (EDS), X-ray diffractometer (XRD), potentiodynamic polarization curve (PPC), electrochemical impedance spectroscopy (EIS), optical microscope (OM), tensile strength test, double shear strength test and tension fatigue test. The test results showed that, compared with industrial atmosphere environment, high-strength bolt exhibited higher corrosion susceptibility in marine atmosphere environment. Lepidocrocite and goethite were the major constituents of the rust layer in two types of atmosphere environments, and chlorides and sulphates were detected in marine atmosphere environment and industrial atmosphere environment, respectively. Electrochemical corrosion analysis showed that the anti-corrosive properties of different parts were in this order: screw part > thread part > joint between thread and screw, resulting that the corrosion extent of the screw part was the lightest among three parts. The results of mechanical properties test indicated that the tension fatigue life decreased distinctly with the prolongation of the exposure time in two types of atmosphere environments, and the losses in tension fatigue life of 1Cr17Ni2 high-strength bolt exposed in marine atmosphere environment was much larger than that of 1Cr17Ni2 high-strength bolt exposed in industrial atmosphere environment. Tensile strength and double shear strength did not present visible decrease during the exposure time of 36 months.

Keywords: high-strength bolt; atmospheric corrosion; marine and industrial atmosphere environments; mechanical properties

1. INTRODUCTION

Bolt, which is the most commonly employed standard parts, has been widely used as connection

parts in the fields of automobile, building, aviation, etc. [1]. In those fields, bolt is usually exposed in various outdoor atmosphere environments and could be affected by corrosion attack, then resulting in the decrease in mechanical properties. The accidents caused by the corrosion fracture of metal bolt occur frequently in service, many countries pay more and more attention to the studies on the atmospheric corrosion and properties degradation of the metal bolt [2, 3].

The atmospheric corrosion performance of products can be evaluated with the method of laboratory test or field exposure test. The laboratory test is particularly useful for the study of the corrosion mechanism and obtaining the influence of specific pollutants and ions on products, but has limited value for predicting actual service performance. It is well known that the field exposure test provides actual information on the corrosion of the products, and it is the most important method for investigating atmospheric corrosion [4–13].

1Cr17Ni2 high-strength bolt, which is one of the most widely used stainless bolt due to its excellent corrosion resistance, high strength and high-temperature resistance, has been extensively used as the important connection and bear-force parts in the aerospace industry [1]. The atmospheric corrosion performance of 1Cr17Ni2 high-strength bolt has an important bearing on the service safety and product life. Some researchers have been done and reported on the corrosion behavior of 1Cr17Ni2 stainless steel materials, whose western counterparts is grade AISI 431, by dint of laboratory test, and the meaningful results have been obtained [14,15]. However, to our best knowledge, little published information is available about field exposure test done with 1Cr17Ni2 stainless steel, especially 1Cr17Ni2 high-strength bolt, whose information on the corrosion behavior in representative atmosphere environments plays more important value and possesses more direct role to the designer of manufacture than that of 1Cr17Ni2 stainless materials. In view of the representativeness, the extensive applications and the advantages of field exposure test, extensive long-term corrosion evaluation of 1Cr17Ni2 high-strength bolt in different atmosphere environments needs to be conducted and reported.

The aim of this research is to investigate the atmospheric corrosion behaviour of 1Cr17Ni2 high-strength bolt exposed both in marine and industrial atmosphere environments, and understand the evolution of corrosion morphologies, corrosion product, tensile strength, double shear strength and tension fatigue. This work can provide useful references for the expansion of its applications, the design of corrosion protection and development of new types of high-strength bolt.

2. EXPERIMENTAL

2.1 Materials preparation

The chemical composition of 1Cr17Ni2 high-strength bolt was listed in Table 1, which was in accord with GJB 2294A standard [16]. The 1Cr17Ni2 high-strength bolt with a size specification of 10 mm×50 mm was manufactured according to the HB 7411 standard [17], and the surface was treated by passivation process based on HB 5292 standard [18].

Table 1. Chemical compositions of 1Cr17Ni2 high-strength bolt

Element	C	Si	Mn	P	S	Cr	Ni	Fe
Composition (wt.%)	0.11~ 0.17	≤0.8	≤0.8	≤0.03	≤0.025	16~18	1.5~2.5	Bal.

2.2 Atmospheric exposure tests

Atmospheric exposure tests were undertaken at Wanning natural environmental test site and Jiangjin natural environmental test site, which represented the marine atmosphere environment and industrial atmosphere environment, respectively. The environmental factors, whose measurement was on the basis of ISO 9225 [19] and GB/T 24516.1 standards [20], are listed in Table 2. According to ISO 8565 standard [21], the samples were exposed in direction to south at an angle of 45° from the horizon under open conditions (no roof) at the test sites. The exposure location at Wanning natural environmental test site was 375 m from the shoreline. Fourteen samples were retrieved from each test site for analyses after 6, 12, 18, 24 and 36 months of exposure for each test period. Two of the samples were used to study the surface morphologies and compositions of the corrosion product, and the other twelve samples were used for mechanical properties measurement.

Table 2. Annual averages of meteorological factors and corrosive species at test sites

Test sites	Wanning	Jiangjin
Average temperature (°C)	24	18
Average relative humidity (%)	85	82
Rainfall (mm)	2269	939
Sunshine duration (h)	1954	1487
Humidity duration above 80% (h)	6736	5304
Sulfur dioxide (mg/(100cm ² •d))	0.089	0.330
Airborne sea-salt (mg/(100cm ² •d))	0.200	0.008
Nitrogen dioxide (mg/(100cm ² •d))	0.012	0.022
Sulfureted hydrogen (mg/(100cm ² •d))	0.002	0.002
Ammonia (mg/(100cm ² •d))	0.012	0.070
Hydrochloric acid (mg/m ³)	0.030	0.020

2.3 Corrosion product analysis

The surface micromorphologies and compositions of the corrosion product were studied using Quanta 200 environmental scanning electron microscope (FEI Co., Ltd., the Netherlands) coupled with INCA energy dispersive analyser system (Oxford Co., Ltd., Britain). The cross section morphologies of corroded samples were studied using optical microscope. The phase structure of the corroded samples was analyzed by X-ray diffractometer (BRUKER AXS Co., Ltd., Germany) operating at 40 kV and 40 mA with Cu K_{α} radiation.

2.4 Electrochemical corrosion tests

Electrochemical corrosion tests, which consisted of potentiodynamic polarization curve (PPC) and the electrochemical impedance spectroscopy (EIS), were carried out using a classical three electrodes cell with platinum as counter electrode, saturated calomel electrode SCE (+0.242V vs SHE) as reference electrode, and 1Cr17Ni2 high-strength bolt as working electrode. Three local regions including thread part (containing the bottom area), joint between thread and screw part, screw part were selected as electrochemical test area. The height of test region is 10 mm, and the rest was sealed by the processed polytetrafluoroethylene ring and silicone rubber, as shown in Fig.1. According to the calculation results based on GB/T 5267 standard [22], the test area of thread part (containing the bottom area), joint between thread and screw part, screw part were 561.1mm², 398.6mm² and 314.2mm², respectively.

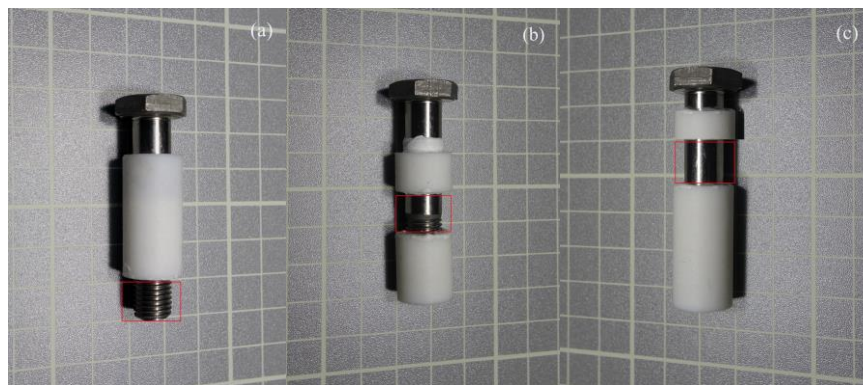


Figure 1. Photos of electrochemical measurement samples with different test regions (a) thread part, (b) joint between thread and screw part, (c) screw part.

The neutral 5.0 wt.% NaCl solution (open to air at 20±2 °C) was used as corrosive media. The PAR system, which included a M263A potentiostat, a M5210 lock-in amplifier and the PowerSuite software, was used for measuring the PPC and the EIS. The constant voltage scan rate for PPC test was 0.1 mV s⁻¹. The employed amplitude of sinusoidal signal for EIS test was 10 mV, and the frequency range studied was from 10⁵ to 10⁻² Hz. The acquired EIS data were curve fitted and analyzed using *ZsimpWin 3.20* software. All the corrosion tests were normally repeated three times under the same conditions, checking that they presented reasonable reproducibility.

2.5 Mechanical properties tests

The tensile strength, double shear strength and tension fatigue life of 1Cr17Ni2 high-strength bolt were test based on the GJB 715.23 A [23], GJB 715.26 A [24] and GJB 715.30A [25], respectively. The reported value of each mechanical property was derived from the average of four parallel samples.

3. RESULTS AND DISCUSSION

3.1 Surface morphologies analysis

The typical surface macromorphologies of 1Cr17Ni2 high-strength bolt exposed in marine atmosphere environment and industrial atmosphere environment with the prolongation of the exposure time are shown in Fig. 2 and Fig. 3, respectively. It can be seen that the corrosion extent of 1Cr17Ni2 high-strength bolt increased with the prolongation of the exposure time in two types of atmosphere environments. Clearly, the corrosion degree of 1Cr17Ni2 high-strength bolt exposed in marine atmosphere environment was more serious than that of 1Cr17Ni2 high-strength bolt exposed in industrial atmosphere environment, which attributed to the high chloride ion concentration in marine atmosphere environment and the strong penetration effect of chloride on the passive film formed on the stainless steel. What was interesting in industrial atmosphere environment was that the corrosion phenomena occurred hardly in the whole screw of 1Cr17Ni2 high-strength bolt, which would be explained by dint of electrochemical method in the following section of electrochemical corrosion analysis.



Figure 2. Typical surface macromorphologies of 1Cr17Ni2 high-strength bolt exposed in marine atmosphere environment (Wanning) for (a) 12 months, (b) 24 months and (c) 36 months



Figure 3. Typical surface macromorphologies of 1Cr17Ni2 high-strength bolt exposed in industrial atmosphere environment (Jiangjin) for (a) 12 months, (b) 24 months and (c) 36 months

The observation localization for micromorphologies was the joint between thread and screw part (as shown in Fig.1b), in which the fracture position of 1Cr17Ni2 high-strength bolt concentrated during the tensile strength test and the tension fatigue test. The typical surface micromorphologies of the joint

between thread and screw part for 1Cr17Ni2 high-strength bolt exposed in marine and industrial atmosphere environments with the prolongation of the exposure time are shown from Fig. 4 to Fig. 14. To all appearances, surface micromorphologies of the rust layer not only took on considerable diversity among different atmosphere environments, but also varied with the prolongation of the exposure time at a given atmosphere environment. The rust layer most frequently found presented typical shape or structures which can be classified into several main types of morphologies: globular, acicular, laminar, tubular and toroidal. The terms aforementioned to describe rust morphologies were coined by Morcillo et al. in their latest publications in which the SEM/Micro-Raman spectroscopy technique with more scientificity and reliability was employed to investigate the rust phase and corresponding morphologies or structures [26-28]. The constituents of the rust layer aftermentioned were estimated mainly on the basis of the corresponding relationship between the types of micromorphologies and the types of constituents, which have been discussed in the past literatures [5, 6, 10, 13, 26-29].

The typical surface micromorphologies of the screw for the joint between thread and screw part exposed in marine atmosphere environment are shown from Fig. 4 to Fig. 6. It can be seen from Fig. 4 that rust layer of the screw mainly presented petaloid and granulated morphologies which were the characteristics of goethite (α -FeOOH) and lepidocrocite (γ -FeOOH), respectively. With the exposure time of 24 months, as shown in Fig. 5, the morphologies with the shape of granula, threadiness and spherality, which were the characteristic of lepidocrocite (γ -FeOOH), were observed. Under much higher magnification, as shown in Fig. 5b, the needles (whiskers) formations around the periphery of the globules was actually observed, indicating the existence of goethite (α -FeOOH) which formed by the transformation of lepidocrocite (γ -FeOOH).

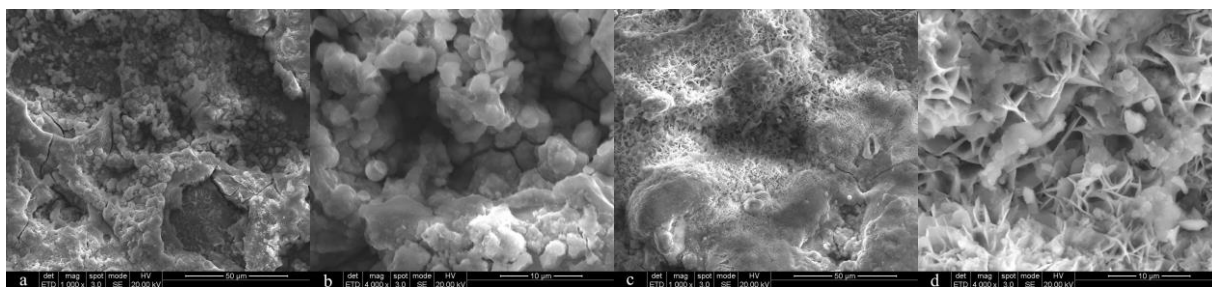


Figure 4. Typical surface micromorphologies of screw for joint between thread and screw part in marine atmosphere environment for 12 months

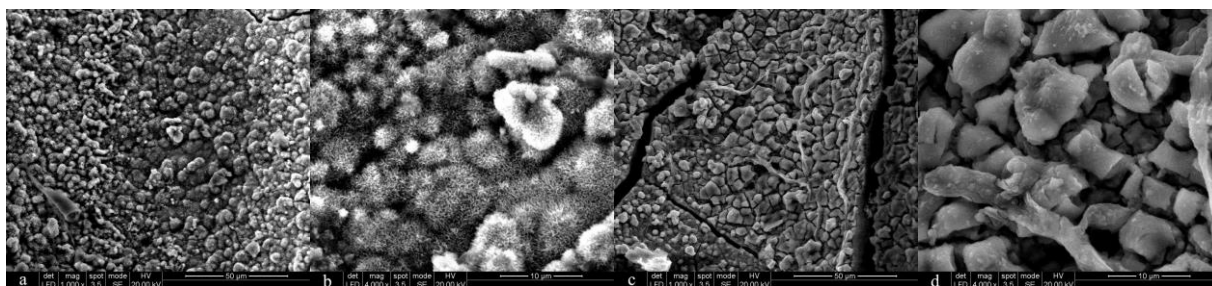


Figure 5. Typical surface micromorphologies of screw for joint between thread and screw part in marine atmosphere environment for 24 months

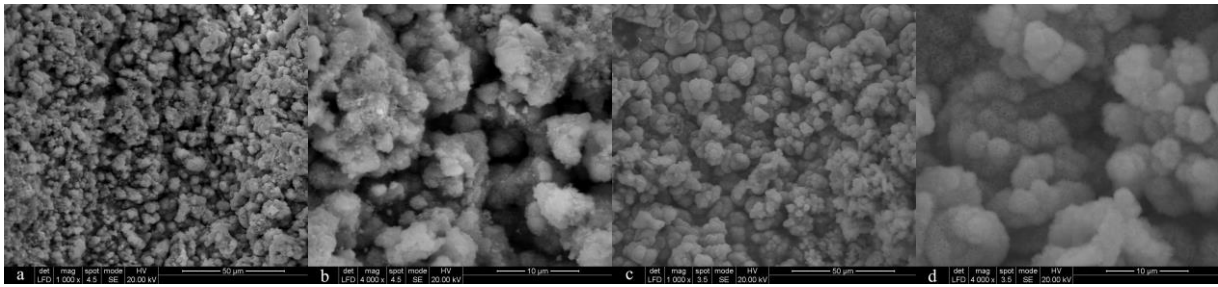


Figure 6. Typical surface micromorphologies of screw for joint between thread and screw part in marine atmosphere environment for 36 months

When the exposure time was 36 months, as shown in Fig.6, the rust layer of the screw mainly presented granulated morphologies, which were the characteristic of lepidocrocite (γ -FeOOH).

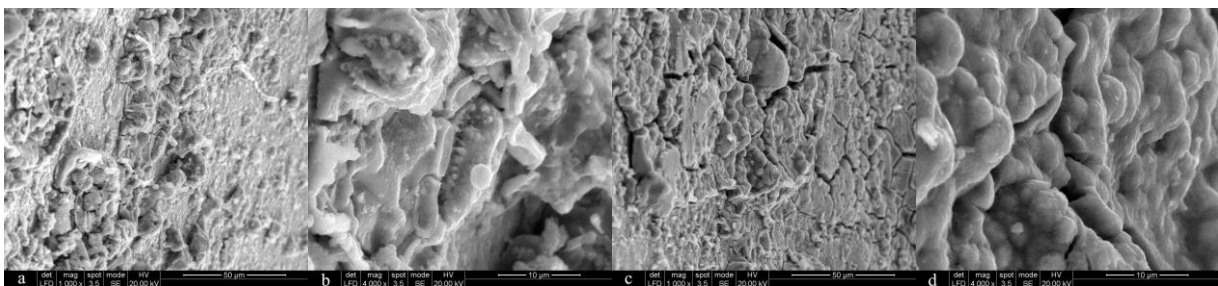


Figure 7. Typical surface micromorphologies of thread for joint between thread and screw part exposed in marine atmosphere environment (Wanning) for 12 months

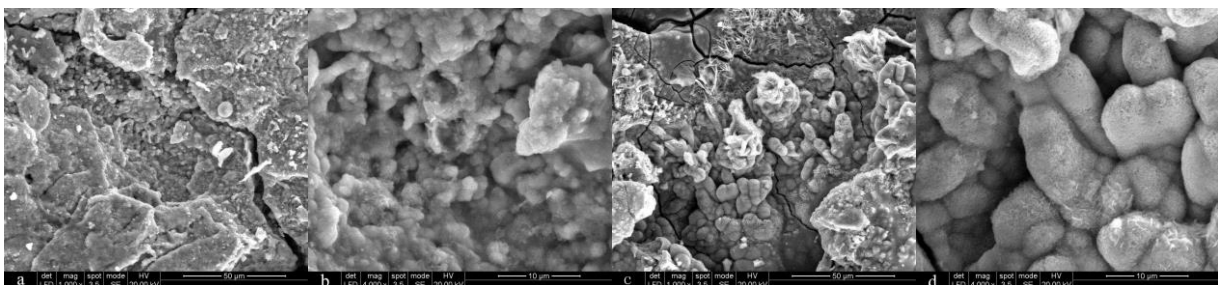


Figure 8. Typical surface micromorphologies of thread for joint between thread and screw part exposed in marine atmosphere environment (Wanning) for 24 months

The typical surface micromorphologies of the thread for the joint between thread and screw part exposed in marine atmosphere environment are shown from Fig. 7 to Fig. 9. From Fig.7 it can be seen that rust layer of thread mainly presented cellular morphologies which was the characteristic of lepidocrocite (γ -FeOOH). With the exposure time of 24 months, as shown in Fig.8, the morphologies with the shape of granula and spherality, which were the characteristic of lepidocrocite (γ -FeOOH), were observed. Under much higher magnification as shown in Fig.8d, the needles (whiskers) formations around the periphery of the globules was actually observed, indicating the existence of goethite (α -

FeOOH). When the exposure time was 36 months, as shown in Fig.9, the rust layer of the thread mainly presented granulated and feather-like morphologies, which were the characteristic of lepidocrocite (γ -FeOOH). The microcrack always occurred in rust layer during the exposure time.

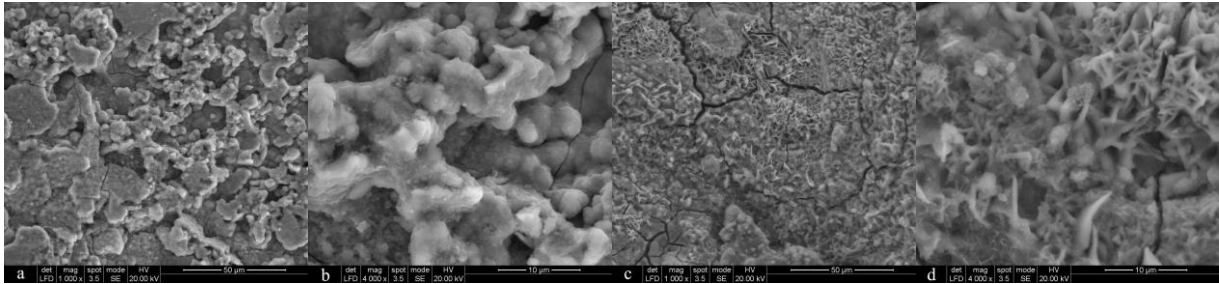


Figure 9. Typical surface micromorphologies of thread for joint between thread and screw part exposed in marine atmosphere environment (Wanning) for 36 months

The Typical EDS plots of the joint between thread and screw part exposed in marine atmosphere environment, as shown in Fig.10, revealed the existence of chlorine element, indicating reasonably that the existence of the water-soluble compounds such as ferrous chloride (FeCl_2) and ferric chloride (FeCl_3).

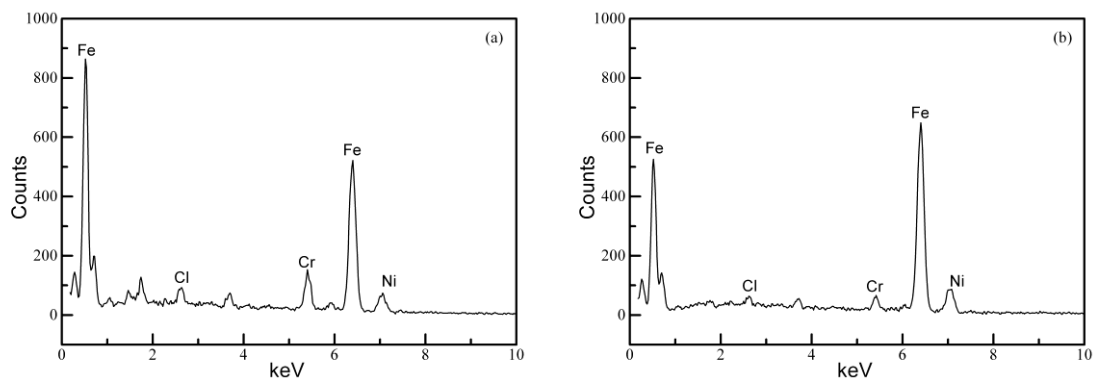


Figure 10. Typical EDS plots of joint between thread and screw part exposed in marine atmosphere environment (Wanning) for 36 months (a) thread, (b) screw

From the surface micromorphologies analysis of the rust layer formed in marine environmental atmosphere, it can be concluded that lepidocrocite and goethite were found as the major constituents of the rust layer. Ferrous chloride and ferric chloride, whose shape or structure were barely studied and reported, were also detected as the constituents of the rust layer. The water-soluble compounds have been analyzed and reported on the outdoor exposure test of metallic materials by Oesch and Heimgartner [30]

The typical surface micromorphologies of the thread for the joint between thread and screw part exposed in industrial atmosphere environment are shown from Fig. 11 to Fig. 13. From Fig.11 it can be seen that the rust layer of the thread was compact, and mainly presented cellular and muddy

morphologies which were the characteristic of lepidocrocite (γ -FeOOH). With the exposure time of 24 months, as shown in Fig.12, the morphologies with the shape of granula, which were the characteristic of lepidocrocite (γ -FeOOH), were observed. The tubulous morphologies indicating the existence of goethite (α -FeOOH) were also observed. When the exposure time was 36 months, the morphologies with the shape of granula and threadiness, which were the characteristic of lepidocrocite (γ -FeOOH), were observed.

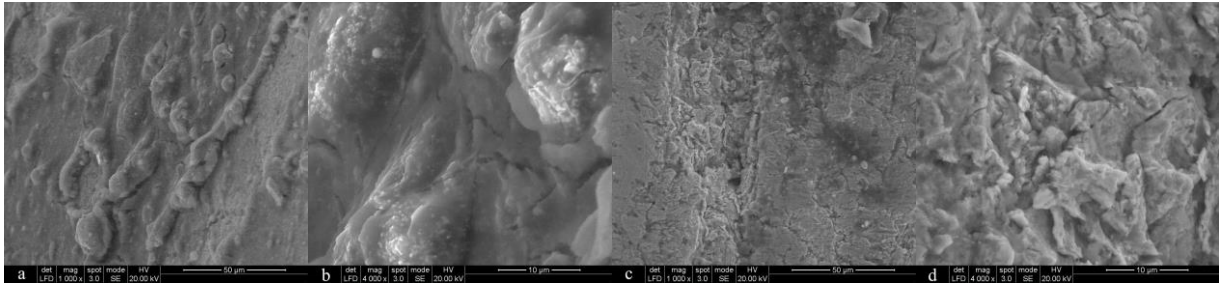


Figure 11. Typical surface micromorphologies of thread for joint between thread and screw part exposed in industrial atmosphere environment (Jiangjin) for 12 months

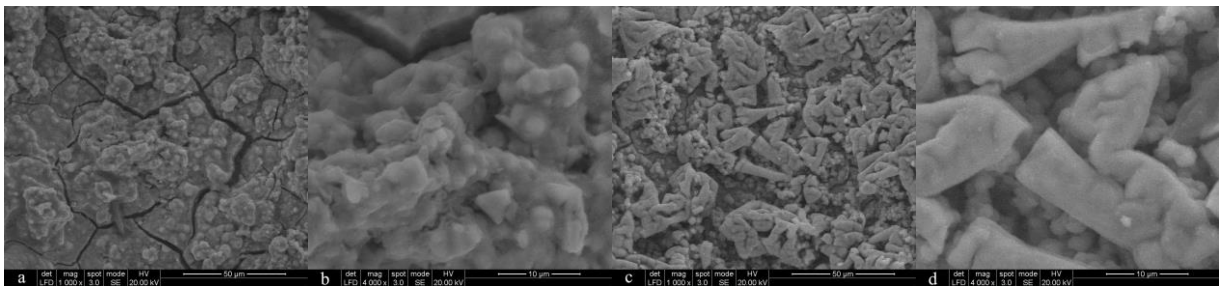


Figure 12. Typical surface micromorphologies of thread for joint between thread and screw part exposed in industrial atmosphere environment (Jiangjin) for 24 months

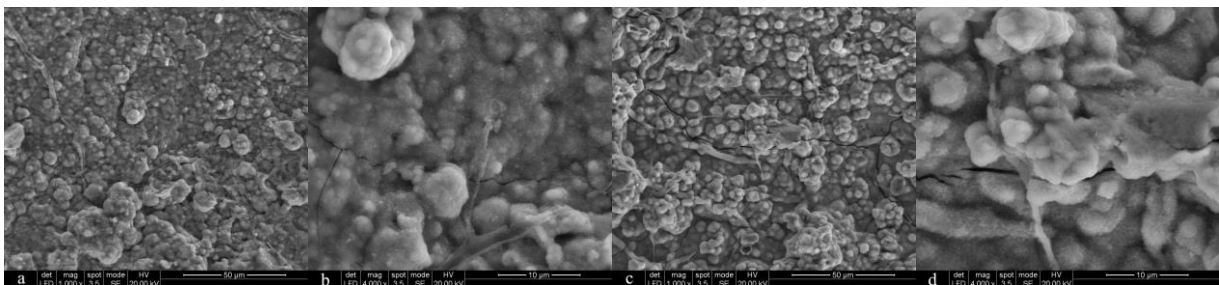


Figure 13. Typical surface micromorphologies of thread for joint between thread and screw part exposed in industrial atmosphere environment (Jiangjin) for 36 months

The Typical EDS plots of the thread for joint between thread and screw part exposed in industrial atmosphere environment, as shown in Fig.14, revealed the existence of sulfur element, indicating reasonably the existence of ferrous sulphate (FeSO_4) and ferric sulphate ($\text{Fe}_2(\text{SO}_4)_3$).

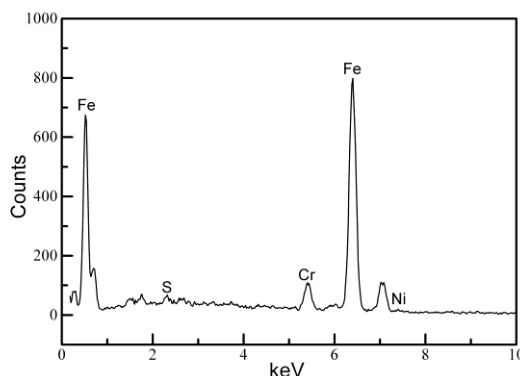


Figure 14. Typical EDS plots of thread for joint between thread and screw part exposed in industrial atmosphere environment for 36 months

On the basis of the micromorphologies analysis of the rust layer formed in industrial atmosphere environment, it can be concluded that lepidocrocite and goethite, which were frequently found in atmospheric corrosion products of steel, were the major constituents of the rust layer. Ferrous sulphate and ferric sulphate, whose shape or structure were barely studied and reported, were also detected as the constituents of the rust layer.

Furthermore, the rust layer in two types of atmosphere environments all appeared the cracks, which was often the case occurred on the surface of rust layer. Compared the rust layer in industrial atmosphere environment, the rust layer in marine atmosphere environment showed more open surface structure indicating a low protective power, which did not effectively prevent aggressive environmental agents from reaching the base steel, thus also explaining the high corrosion susceptibility of 1Cr17Ni2 high-strength blot in marine atmosphere environment.

3.2 XRD analysis

The crystalline phases of the rust layer in two types of atmosphere environments with the exposure time of 12 months and 36 months are shown in Fig. 15. It can be seen from Fig.15 that the rust constituents in marine atmosphere environment and industrial atmosphere environment were quite similar, and were mainly composed of goethite (α -FeOOH) and lepidocrocite (γ -FeOOH). The nature of the rust constituents wasn't affected with the prolongation of the exposure time in two types of atmosphere environments, and the same species were always detected at a given atmosphere environment.

It was interesting to note that, when the exposure time was 36 months, the goethite (α -FeOOH) was not observed in two types of atmosphere environments which can be seen from the surface micromorphologies analysis. It seemed to be in contradiction with the XRD analysis. The occurrence of phenomenon mentioned above can be attributed that lepidocrocite (γ -FeOOH) was primarily present in external surface of the layer and was the most abundant when observing the external surface of the

rust layer [31].

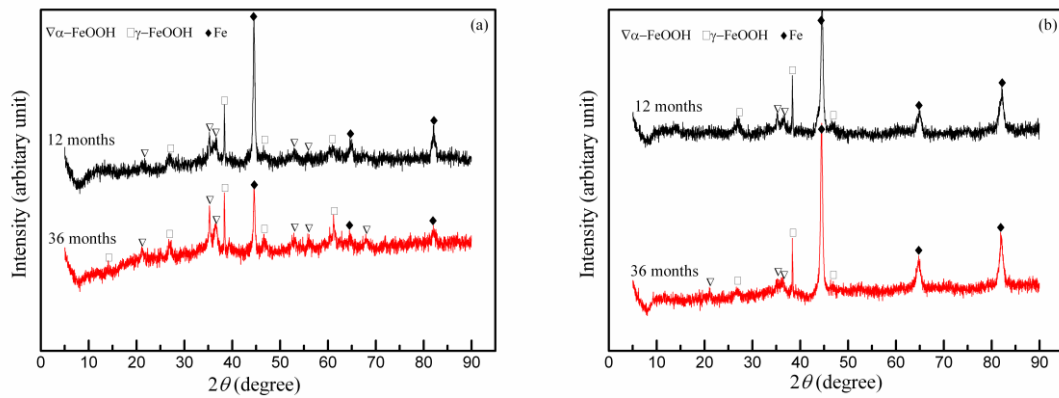


Figure 15. XRD patterns of rust layer (a) Wanning, (b) Jiangjin

3.3 Electrochemical corrosion analysis

Typical potentiodynamic polarization curves of three test regions in neutral 5.0 wt. % NaCl solution are presented in Fig.16. Corrosion current density (i_{corr}) derived from Fig.16 using the Tafel extrapolation is also summarized. It can be found that the i_{corr} of the screw part is $4 \times 10^{-7} \text{ A cm}^{-2}$, which is respectively approximately 1/15 and 1/50 that of the thread part and that of the joint between thread and screw part, suggesting the best corrosion resistance of the screw part among three test regions.

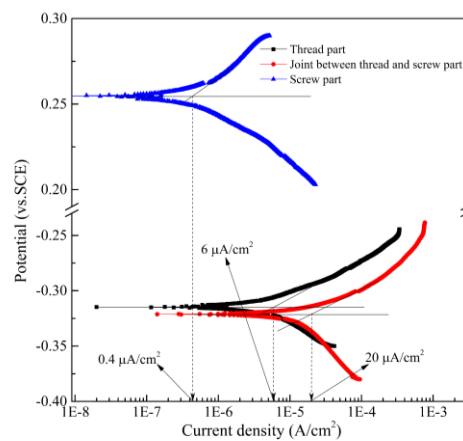


Figure 16. Typical potentiodynamic polarization curves of three test regions in neutral 5.0 wt. % NaCl solution

The typical electrochemical impedance spectroscopy of the different test regions in neutral 5.0 wt.% NaCl solution are presented in Fig.17. A low-frequency inductive loop, whose shape was characterized with retractile real part, was observed in the Nyquist plots of the three test regions. The appearance of the low-frequency inductive loop may originate from the pitting corrosion on the electrode surface [32]. It can be seen from Fig. 17a that the diameters of capacitance loop were in this order: screw part > thread part > joint between thread and screw part, indicating the highest corrosion resistance of screw part among three test regions. From the Bode plots (impedance modulus $|Z|$) as a function of

frequency), as shown in Fig.17b, it can be detected that the impedance value of three test regions was also in this order: screw part > thread part > joint between thread and screw part. The changes of the Bode plots (phase angle as a function of frequency) , as shown in Fig.17c, indicated that there was only one time constant for three test regions in 5.0 wt. % NaCl solutions over the whole frequency range studied, which reflected one relaxation process, i.e. dissolution of working electrode during the corrosion process.

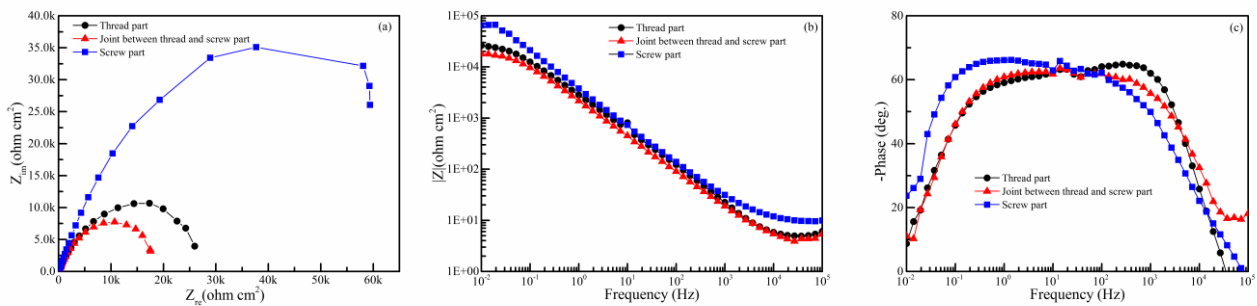


Figure 17. Typical electrochemical impedance spectroscopy of three test regions in neutral 5.0 wt. % NaCl solution (a) Nyquist plots, (b and c) Bode plots

In order to further and quantitatively study the corrosion process of three test regions, a more detailed interpretation of EIS measurement is performed by fitting the experimental plots using the electrochemical equivalent circuit depicted in Fig. 18.

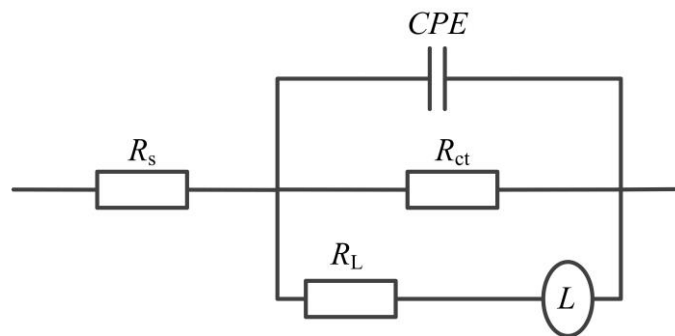


Figure 18. Electrochemical equivalent circuits used for fitting EIS data of three test regions in neutral 5.0 wt. % NaCl solution

The circuit, presented in Fig.18, consisted of parameters namely solution resistance (R_s), charge transfer resistance (R_{ct}), inductance resistance (R_L), inductance (L) and a constant phase element (CPE) which replaces the capacitance of the double layer (C_{dl}). A constant phase element (CPE) replaces the capacitance of the double layer (C_{dl}) due to the roughness and inhomogeneity of the electrode surface.

The impedance of CPE is given by the following equation [32, 33]:

$$Z_{CPE}(\omega) = Y_0^{-1} (j\omega)^{-n} \quad (1)$$

Where Y_0 is a constant that is independent of frequency, ω is angular frequency, $j = \sqrt{-1}$ and n is exponential index which represents a dispersion of relaxation. When n equals 0, CPE acts as a pure

resistor; when n equals 1, CPE represents an ideal capacitor; when n equals -1, CPE possesses the characteristic of inductance. The impedance of L could be described as follows:

$$Z_L(\omega) = j\omega L \quad (2)$$

Charge transfer resistance (R_{ct}) is the resistance offered by the metal atom to get ionized when in contact with the electrolyte. The higher charge transfer resistance, the better corrosion resistance. The fitted values of the R_{ct} with regard to joint between thread and screw part, thread part and screw part in neutral 5.0 wt. % NaCl solution are $19320 \Omega \cdot \text{cm}^2$, $26500 \Omega \cdot \text{cm}^2$ and $79600 \Omega \cdot \text{cm}^2$, respectively.

From the corrosion analysis by dint of EIS, it can be seen that screw part presented the best corrosion resistant in three test regions, which was consistent with the potentiodynamic polarization analysis.

Considering of the comprehensive test results of potentiodynamic polarization and electrochemical impedance spectroscopy, it can be concluded that the corrosion resistance of three test regions was in this order: screw part > thread part > joint between thread and screw part. The corrosion resistance of screw part was much greater than that of thread part. Furthermore, although the corrosion resistance of thread part was higher than that of joint between thread and screw part, the difference was not distinct, which can be concluded from the corrosion current density (i_{corr}) and charge transfer resistance (R_{ct}). The analysis mentioned above can be used to explain that the corrosion phenomena occurred hardly in the whole screw of 1Cr17Ni2 high-strength bolt exposed in industrial atmosphere environment.

3.4 Cross section morphologies analysis

The observation localization for cross section morphologies was the thread for the joint between thread and screw part, in which the fracture position of 1Cr17Ni2 high-strength bolt concentrated during the tension fatigue test. Furthermore, the tension fatigue life of 1Cr17Ni2 high-strength bolt decreased obviously with the prolongation of the exposure time, which would be described in the section of mechanical properties analysis.

The typical cross section morphologies of thread for the joint between thread and screw part of 1Cr17Ni2 high-strength bolt exposed in marine atmosphere environment and industrial atmosphere environment with the exposure time of 36 months are shown in Fig. 19 and Fig. 20, respectively. Obviously, the corrosion area and the corrosion depth of thread in marine atmosphere environment were greater than that of thread in industrial atmosphere environment.

Furthermore, the thickness of the rust layer was quite uneven. According to the study reported by Asami and Kikuchi [34], there can be no argument that the origin of unevenness came from the non-uniform distribution of physical and chemical factors, such as environmental deposits and the direction of crystallites in the steel.

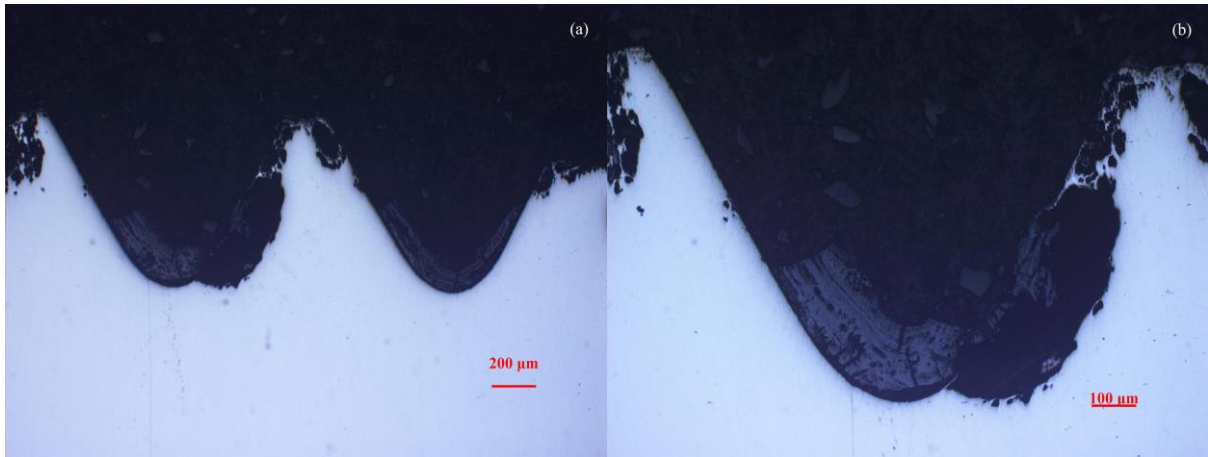


Figure 19. Cross section morphologies of thread for joint between thread and screw part exposed in marine atmosphere environment (Wanning) for 36 months

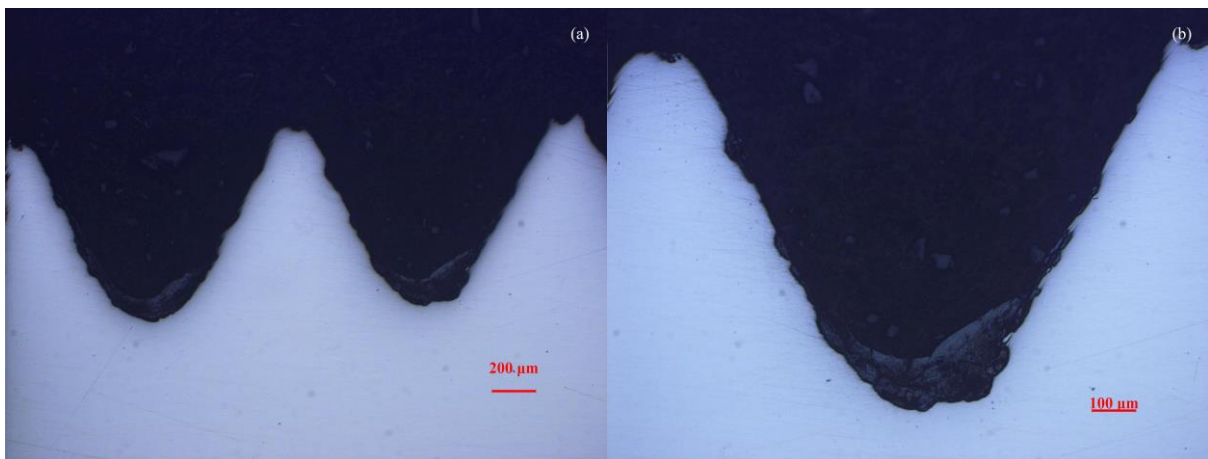


Figure 20. Cross section morphologies of thread for joint between thread and screw part exposed in industrial atmosphere environment (Jiangjin) for 36 months

3.5 Mechanical properties analysis

The losses in mechanical properties of 1Cr17Ni2 high-strength bolt with the prolongation of the exposure time at two test sites are shown in Fig. 21. Apparently, the losses in tension fatigue life of 1Cr17Ni2 high-strength bolt were distinct, and the losses in tension fatigue life increased with the prolongation of the exposure time. However, the double shear strength and tension strength fluctuated during the whole exposure time, and the fluctuant extent limited the scope of 5% compared with the original properties value. This indicated that the corrosion on the surface of 1Cr17Ni2 high-strength bolt and the etch pits has no obvious effect on the double shear strength and tension strength after the exposure time of 36 months.

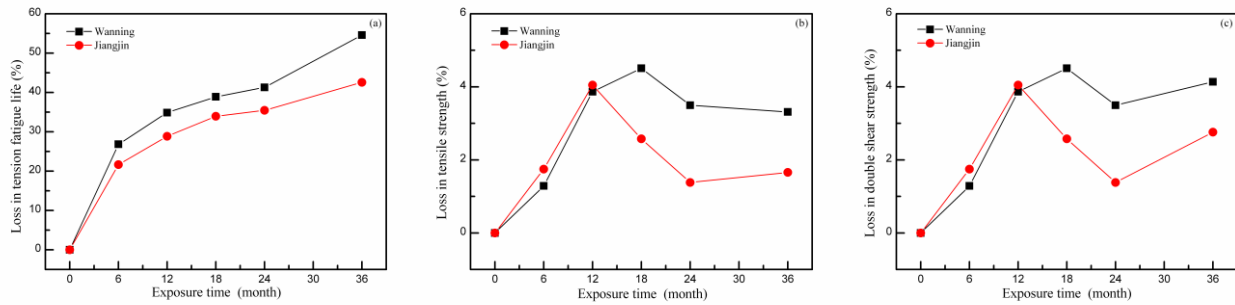


Figure 21. Losses in mechanical properties for 1Cr17Ni2 high-strength bolt versus exposure time at two test sites (a) tension fatigue life, (b) tensile strength and (c) double shear strength.

From the cross section morphologies analysis mentioned above, it can be seen that some etch pits occurred in two types of atmosphere environments, especially the root of thread, along which crack initiation was prone to propagate, resulting the decreases in tension fatigue life. The losses in tension fatigue life of 1Cr17Ni2 high-strength bolt in marine atmosphere environment were larger than that of 1Cr17Ni2 high-strength bolt in industrial atmosphere environment, which can be attributed to the corrosion extent of thread exposed in marine atmosphere environment was larger than that of thread exposed in industrial atmosphere environment, as shown in Fig. 19 and Fig. 20. After 36 months of exposure test, the losses in tension fatigue life of 1Cr17Ni2 high-strength bolt in marine atmosphere environment and industrial atmosphere environment were 55% and 43%, respectively.

4. CONCLUSIONS

Compared with marine atmosphere environment, high-strength bolt exhibited lighter corrosion susceptibility in industrial atmosphere environment. The corrosion extent of the screw part was the lightest among three parts, which attributed the corrosion current density (i_{corr}) of the screw part was much smaller than that of the other parts, and charge transfer resistance (R_{ct}) of the screw part was much larger than that of the other parts.

The lepidocrocite and goethite were found to be the major constituents of the rust layer in two types of atmosphere environments. Chlorides and sulphates were also detected in marine atmosphere environment and industrial atmosphere environment, respectively.

The tension fatigue life of high-strength bolt exposed in marine atmosphere environment was much shorter than that of high-strength bolt exposed in industrial atmosphere environment, which can be attributed that the corrosion extent of high-strength bolt exposed in marine atmosphere environment was evidently larger than that of high-strength bolt exposed in industrial atmosphere environment.

Tensile strength and double shear strength of high-strength bolt did not presented visible decrease with the exposure time of 36 months, although the corrosion phenomena of high-strength bolt occurred in two types of atmosphere environments.

ACKNOWLEDGEMENTS

The authors gratefully acknowledge the financial support of National Technology Foundation Program (JSJC2013209B058) and the help rendered by the staff of the natural environmental test sites in this work.

References

1. Z.X. Jiang, Z.F. Xu, T. Zhang, Preparation and Failure Cases of Fasteners, National Defence Industry Press, 2015.
2. C.J. Yu, G.Q. Huang, *Equip. Environ. Eng.*, 7 (2010) 4.
3. X.L. Yang, J.M. Zhang, Y.G. Chen, *J. Nanjing Univ. Aeronaut&Astronaut.*, 41 (2009) 130.
4. S. Syed, *Mater. Corrosion*, 61 (2010) 238.
5. D. de la Fuente, I. Díaz, J. Simancas, B. Chico, M. Morcillo, *Corros. Sci.*, 53 (2011) 604.
6. J.G. Castaño, C.A. Botero, A.H. Restrepo, E.A. Agudelo, E. Correa, F. Echeverría, *Corros. Sci.*, 52 (2010) 216.
7. Q.C. Zhang, J.S. Wu, J.J. Wang, W.L. Zheng, J.G. Chen, A.B. Li, *Mater. Chem. Phys.*, 77 (2002) 603.
8. Z.Y. Cui, X.G. Li, K.Xiao, C.F. Dong, Z.Y. Liu, D.W. Zhang, *Corros. Eng. Sci. Technol.*, 50 (2015) 438.
9. B.B. Wang, Z.Y. Wang, W. Han, W. Ke, *Corros. Sci.*, 59 (2012) 63.
10. X.K. Yang, L.W. Zhang, M. Liu, S.Y. Zhang, K. Zhou, Z.X. She, X.L. Mu, D.F. Li, *Corros. Eng. Sci. Technol.*, 52 (2017) 226.
11. V. Araban, M. Kahram, D. Rezakhani, *Corros. Eng. Sci. Technol.*, 51 (2016) 498.
12. D. de la Fuente, J.G. Castaño and M. Morcillo, *Corros. Sci.*, 49 (2007) 1420.
13. X.K. Yang, L.W. Zhang, S.Y. Zhang, M. Liu, K. Zhou, X.L. Mu, *Mater. Corros.*, 68 (2017) 529.
14. L. Song, *Fail. Anal. Prev.*, 12 (2017) 265.
15. P. Reilhac, J. Creus, X. Feaugas, G. Michel, V. Branger, *J. Mater. Eng. Perform.*, 28 (2019) 3785.
16. GJB 2294A—2014. Specification for stainless and heat-resisting steel bars for aviation, 2014.
17. HB 7411—1996. MJ Hexagon head bolts, 1996.
18. HB 5292—1984. Quality inspection of acid cleaning and passivation for stainless steel, Beijing, 1984.
19. ISO 9225—2012. Corrosion of metals and alloys—corrosivity of atmospheres—measurement of environmental parameters affecting corrosivity of atmospheres, Geneva, 2012.
20. GB/T 24516.1—2009. Corrosion of metals and alloys—atmospheric corrosion—determination of meteorologic factors, 2009.
21. ISO 8565—2011. Metals and alloys – atmospheric corrosion testing—general requirement, 2011.
22. GB/T 5627—2002. Fastener Electroplated Coatings, 2002.
23. GJB 715.23A—2008. Fastener test method—Tensile strength, 2008.
24. GJB 715.26A —2008. Fastener test method—Double shear, 2008.
25. GJB 715.30A—2002. Fastener test method—Tension fatigue, 2002.
26. J. Alcántara, B. Chico, J. Simancas, I. Díaz, D. de la Fuente, M. Morcillo, *Mater. Charact.*, 118 (2016) 65.
27. D. de la Fuente, J. Alcántara, B. Chico, I. Díaz, J.A. Jiménez, M. Morcillo, *Corros. Sci.*, 110 (2016) 253.
28. M. Morcillo, B. Chico, J. Alcántara, I. Díaz, R. Wolthuis, D. de la Fuente, *J. Electrochem. Soc.*, 163 (2016) C426.
29. A. Razvan, A. Raman, *Prakt. Metallogr.*, 23 (1986) 223.
30. S. Oesch, P. Heimgartner, *Mater. Corros.*, 47 (1996) 425.
31. C. Leygraf, T. Graedel, Atmospheric Corrosion, John Wiley & Sons, 2000.

32. C.N. Cao, J.Q. Zhang, *An Introduction of Electrochemical Impedance Spectroscopy*, Science Press, 2002.
33. K. Zhang, B.W. Wen, L.W. Zhang, C. Li, J. Liu, P. Yi, *Int. J. Electrochem. Sci.*, 15 (2020) 11036.
34. K. Asami, M. Kikuchi, *Corros. Sci.*, 45 (2003) 2671.

© 2021 The Authors. Published by ESG (www.electrochemsci.org). This article is an open access article distributed under the terms and conditions of the Creative Commons Attribution license (<http://creativecommons.org/licenses/by/4.0/>).